

Analysis of Air–Turborocket Performance

Giuseppe Bussi,* Guido Colasurdo,† and Dario Pastrone‡
Politecnico di Torino, 10129 Torino, Italy

In order to assess the capabilities of the air–turborocket, an off-design analysis of a representative LOX–LH2 fed engine is carried out. Operating lines are drawn on an advanced compressor map for different flight conditions along the typical flight path of a transatmospheric vehicle. The characteristic aspects of the air–turborocket behavior, in the spontaneous and controlled mode, are highlighted. The full throttle specific thrust and propellant consumption are computed, both in the dry and augmented mode. The performance that can be achieved by exploiting the permissible mass flow range of the compressor map via the variation of the nozzle throat area is shown.

Nomenclature

A	= flow area
F	= thrust
M_0	= flight Mach number
\dot{m}	= air mass flow rate
N_c	= compressor corrected speed
P	= total pressure
q	= dynamic pressure
S	= thrust-specific hydrogen consumption
T	= total temperature
α_n	= nozzle throat area/compressor inlet area
δ	= gas-generator propellant flow rate (referring to the design point value)
η_c	= compressor efficiency
π_c	= compressor total pressure ratio
φ	= hydrogen–air equivalence ratio

Subscripts

dry	= dry mode
max	= maximum allowable in augmented mode
2	= compressor inlet
3	= compressor outlet
4	= turbine inlet
5	= turbine outlet

Introduction

IN literature the term air–turborocket (ATR) does not always refer to the same engine. In the present work, reference is made to the engine that is sketched in Fig. 1. Here, the turbine mass flow is not supplied via the compressor, as in the turbojet engine, but is generated in a separate combustion chamber, or gas generator (GG), which is fed in the same manner as a liquid-propellant rocket engine.^{1–3} The fuel-rich gas from the GG mixes with the compressed airstream after the turbine. Extra fuel is then added, if necessary, and the mixture is burned before expanding in the nozzle.

To the authors' knowledge, few papers^{4–9} have been published on the capabilities and performance of the air–turborocket. Moreover, in these papers attention has mainly been given to the on-design performance of the engine; little

has been said concerning engine control. Yet this problem deserves more attention. Though the turbojet cycle limits are bypassed by independently feeding the turbine via its own gas generator, some ramjet aerothermodynamic limitations and new compressor–turbine matching problems arise. The authors have therefore attempted a description of the off-design behavior as a contribution to the assessment of the capabilities of the air–turborocket, in particular pointing out those limitations that arise because of thermofluidynamics and component matching.

Due to the foreseen applications and according to the aforementioned literature, the analysis has been carried out for a LOX–LH2 fed engine.

Assumptions and Computational Procedures

The best way to highlight the matching problems and to stress the differences between the air–turborocket and the turbojet, is probably to draw the operating lines (i.e., the loci of steady-state matching conditions) on the compressor map. One should, however, remember that in the case of the air–turborocket, there is a particular effect of the flight conditions, i.e., flight Mach number and altitude, on the operating lines, due to the different thermodynamic linkage between the turbine and the compressor, as opposed to the turbojet engine. Whereas a fixed-geometry choked-nozzle turbojet engine presents only one operating line, whose points depend on the fuel throttle, the air–turborocket presents different operating lines for different air inlet total temperatures⁹ [incidentally, the air–turborocket is a “two-lever” engine: the propellant mass flow throttle and the gas-generator mixture ratio (MR) lever; but in this article the MR is held constant]. Each operating line is therefore characterized by the air inlet total temperature that results from the M_0 and the outside static temperature, i.e., from the selected point in the flight path. Therefore, to pose the problem in useful terms, one refers, in this analysis, to a typical flight path,¹⁰ which is shown in Fig. 2. The flight Mach number is associated to each point on the flight path, and the profiles of the compressor inlet

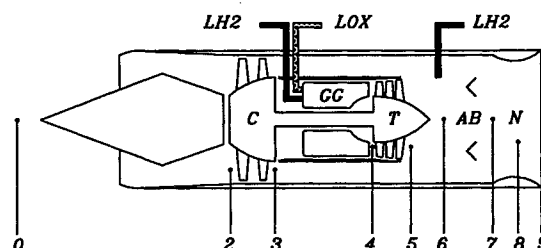


Fig. 1 Air–turborocket schematic diagram: AB = afterburner, C = compressor, GG = gas generator, N = nozzle, and T = turbine.

Presented as Paper 93-1982 at the AIAA/SAE/ASME/ASEE 29th Joint Propulsion Conference, Monterey, CA, June 28–30, 1993; received Oct. 12, 1994; revision received Nov. 16, 1994; accepted for publication Dec. 5, 1994. Copyright © 1993 by the American Institute of Aeronautics and Astronautics, Inc. All rights reserved.

*Professor, Dip. di Energetica, C.so Duca degli Abruzzi 24. Member AIAA.

†Professor, Dip. di Energetica. Member AIAA.

‡Researcher, Dip. di Energetica. Member AIAA.

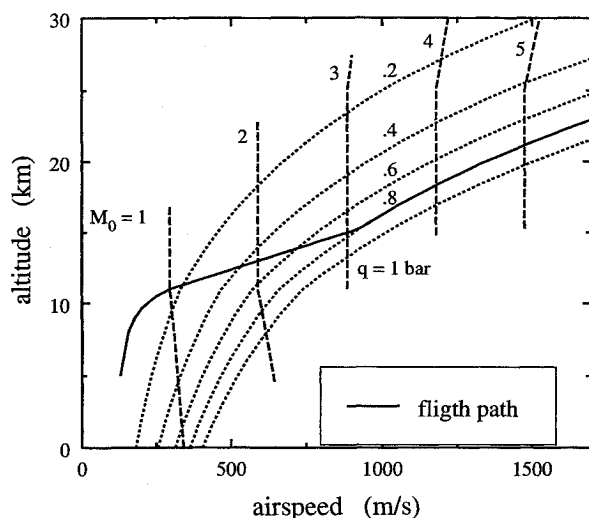


Fig. 2 Flight path.

total temperature and total pressure vs the M_0 can be computed. The intake ram efficiency has been taken into account according to MIL-E-5008B, i.e., $P_2/P_0 = 1$ for $M_0 \leq 1$ and $P_2/P_0 = 1 - 0.075(M_0 - 1)^{1.35}$ for $1 < M_0 < 5$.

Highly sophisticated compressors, using variable pitch to broaden the usable operating range and featuring a rather "elastic" map, have been suggested for this kind of engine. In the present analysis reference is generally made to the operating range of the MTU's HyperCRISP fan¹¹ (a two-stage, counter-rotating, variable-pitch fan). A constant 80% compressor efficiency is assumed for the whole operating range. The maximum mass flow parameter MFP (100%) is established at a 0.6 value.

The assumed LOX-LH2 combination, for the gas-generator propellants, is considered to be the most suitable for aerospace applications. The use of LH2 only, via a regenerative expander cycle, could be interesting and deserves attention; however, the analysis would be more complex, involving the engine dimensions and even possibly the aircraft dimensions. Propellants are burned in a very fuel-rich mixture, in order to restrain the turbine inlet temperature, this not being as essential to the performance as in the turbojet case. The gas-generator temperature $T_4 = 1200 \text{ K}$, corresponding to the mixture ratio $MR = 1.248$ (LOX/LH2, on a mass basis) is assumed on the basis of some suggestions.^{7,8}

Due to this low value of the mixture ratio, the gas flow that meets the air at the turbine exit is essentially made up of some water vapor and a great deal of gaseous hydrogen: the gas from the GG, besides driving the turbine, delivers an initial amount of fuel to the main combustion chamber. The equivalence ratio ϕ_{dry} of the resulting air-gas mixture varies according to the operating conditions and, in some instances, is very large, possibly in excess of one. One can speak of engine dry mode if the combustion is carried out by only exploiting the "natural" input of fuel, i.e., the hydrogen carried by the gas coming out of the turbine. Instead, if extra hydrogen is supplied to the combustion chamber, one can speak of engine-augmented mode. One should note that, as for any airbreathing engine, equivalence ratios above unity result in fuel waste as far as the specific fuel consumption is concerned, while the advantage to the specific thrust is poor.⁷ Therefore, the maximum allowable equivalence ratio due to the extra fuel can be set to one, provided that thermal choking of the burner has not previously been encountered.

A choked turbine is assumed here, with a constant 80% total-to-total efficiency.⁷ The analysis assumes that the turbine outlet total pressure matches the compressor delivery total pressure, $P_5 = P_3$. Propellant pumping work is not accounted for, neither in assessing the engine operating conditions nor

in estimating performance. The pressure losses due to the mixing of the compressor airstream with the gas from the turbine and due to the flameholders are estimated to be 5%. The additional pressure loss due to the heating in the burner is calculated according to the Rayleigh process. The burner flow area is assumed to be equal to the compressor inlet flow area. A variable-throat-area nozzle has been assumed, in order not only to accommodate the thermal choking in the augmented mode, but also as a means of fixing the operating point on the compressor map, i.e., as a further regulation lever.

The variation of the molecular weight due to the combustion is taken into account, but frozen flow is assumed for the airstream and the expanding gases with an appropriate constant heat capacity ratio.

Engine Design Point

The engine has been defined by assuming the following design point data:

- standard sea level static (SSLS)
- compressor pressure ratio: 4
- compressor mass flow parameter (percentage): 95%
- gas-generator pressure: 60 bar

The turbine choked MFP (based on the compressor inlet area) results in a 0.0026 value. The nozzle throat area results to be about 77% of the compressor inlet area.

One should note the fairly high GG pressure level (as suggested for performance reasons), which enhances the turbine specific work, thereby maintaining the ratio of the turbine to the compressor flow at a fairly low value (about 5 and 3%, respectively, on a mass and volume basis). This would undoubtedly imply the necessity of a gear box between the turbine and the compressor.

Operating Lines

Figure 3 shows the aspect and highlights the particular features of the operating lines on the compressor map for the engine geometry that has been established at the aforementioned design point conditions. If one assumes that, at the design conditions, the corrected and mechanical speeds were at their maximum (e.g., 100%), the compressor work must therefore be lowered when the inlet total temperature falls below the SSLS value, while the design point pressure ratio is maintained (this happens for M_0 of less than about 1.3; incidentally, the inlet total pressure also falls below the SSLS value, again reaching this value only at a M_0 of about 1.9).

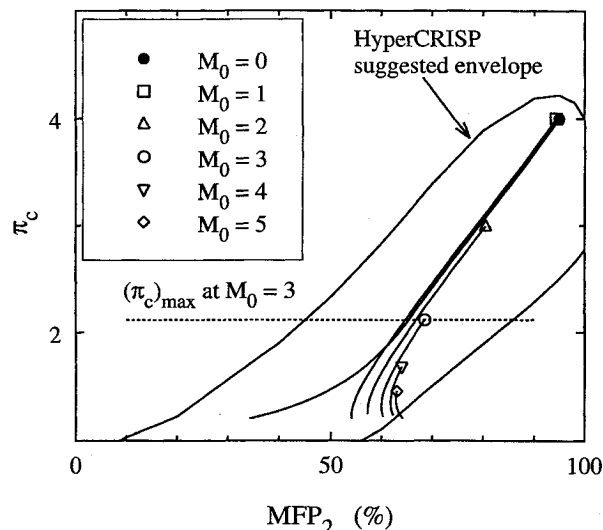


Fig. 3 Operating lines on the fan map.

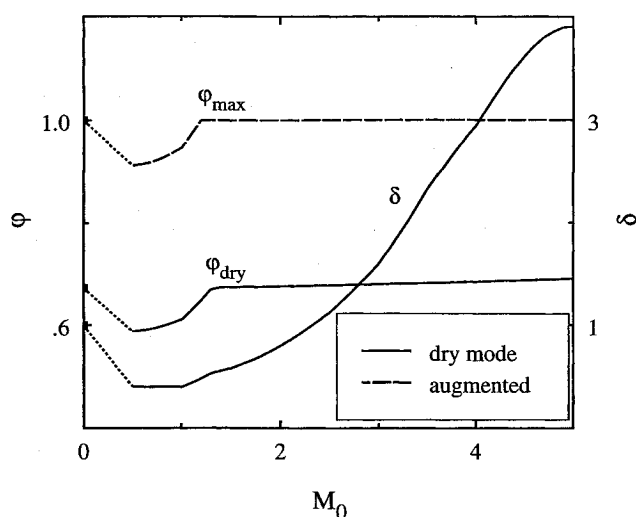


Fig. 4 Full throttle engine parameters.

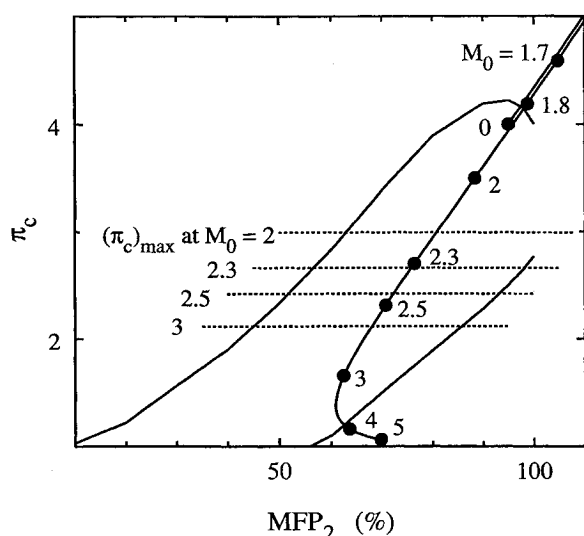


Fig. 5 Spontaneous (constant GG flow) engine behavior.

On the contrary, at higher M_0 , the maximum corrected speed drops, as does the maximum available pressure ratio. In order to highlight this very impressive effect of M_0 on the exploitation of the compressor map (this effect is, however, common to the turbojet engine), the operating lines have been drawn downward from these upper speed limits.

It is worthwhile to consider the amount of the GG propellant necessary to achieve the upper (full throttle) operating point for each M_0 . One may express the GG propellant flow rate as a fraction δ of the design point flow rate; δ also measures the ratio of the required GG pressure to its design point value as the propellant amount is directly proportional to the pressure. As one can deduce from Fig. 4, the required GG pressure varies to a large extent. This could cause some problems as far as the propellant feeding apparatus is concerned.

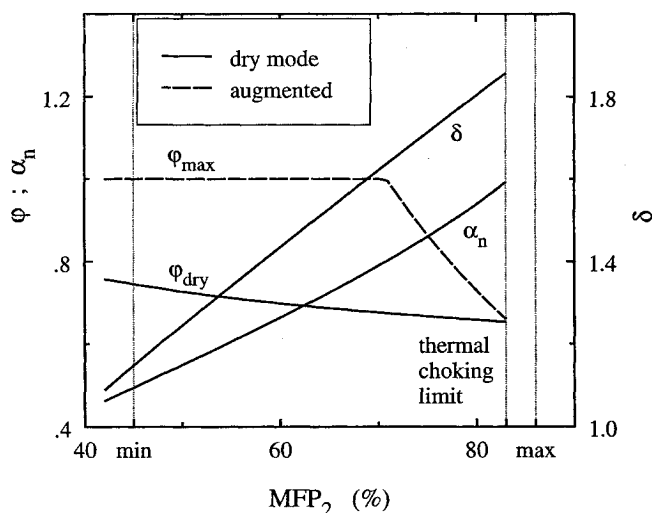
However, even when giving up the aim of reaching the upper operating points, the regulation of the GG propellant mass flow is necessary to some extent. This is perhaps better appreciated if one considers what may be called the "spontaneous behavior of the engine," i.e., the manner in which it responds to variations of the flight conditions, while the propellant flow is kept constant. Figure 5 shows this behavior (one should also note, regarding this aspect, the difference from the turbojet, whose spontaneous behavior is still described by the same operating line as in the controlled mode, while here the compressor-turbine matching results in a new

operating line). As one can see, the compressor speed and mass flow limits are observed only in the M_0 range of about 2.3–3.8 (apart from $M_0 = 0$). At M_0 of less than about 1.8, both the mechanical speed and mass flow limits would be largely exceeded, with a consequent choking of the compressor inlet; on the other hand, compressor internal choking is probably encountered beyond $M_0 = 3.8$.

Figure 4 also shows the ϕ_{dry} yielded by the engine in the dry mode and the maximum allowable ϕ_{max} in the augmented mode. Note that in the transonic region the amount of extra hydrogen in the augmented mode is limited by the occurrence of the afterburner thermal choking.

As shown in Fig. 3, at every M_0 in excess of about 2, the peculiar map of the compressor permits a wide mass flow range, while preserving the pressure ratio at its upper limits. One can take advantage of this favorable feature and largely adjust the operating point on the map by only varying the throat nozzle area (this could also be useful to improve the matching of the engine mass flow with the intake flow capacity). For the purpose of illustrating this aspect, the "cut" at $M_0 = 3$, which is indicated in Fig. 3, is investigated. By moving the operating point on this cut, one obtains the results shown in Fig. 6, where the "min" and "max" limits correspond to the left and right margins of the operating range. Since the compressor work is essentially constant all along the cut, the power that the turbine must deliver increases proportionally to the air mass flow, thus requiring a larger propellant flow, hence a higher GG pressure. However, the propellant flow increases less than proportionally to the airflow, as the turbine work is enhanced by the greater available turbine pressure ratio: the trend of the ϕ_{dry} curve in Fig. 6 is thus explained. The maximum airflow permitted by the map is in this case not achievable, due to the encountered thermal choking limit (the afterburner chokes because its inlet Mach number increases almost proportionally to the airflow rate); however, as one can see, a significant range of airflow variations is available.

In order to highlight what is perhaps the minimum requirement in terms of compressor capabilities, and in order to check the possibility of using a single-stage present-technology fan, the example of Fig. 7 is carried out. For reasons of mechanical matching, only a 20-bar GG pressure is chosen. Some compressor overspeeding, up to 105% of the mechanical speed at takeoff (TO) conditions, seems to be necessary to preserve suitable values of the compressor corrected speed up to about $M_0 = 3$, when the ramjet mode possibly takes over (however, as one can see, the fan is no longer useful for M_0 greater than 3). By adjusting the nozzle area for each M_0 , the operating points are moved to the maximum acceptable air mass flow,

Fig. 6 Engine parameters on the $M_0 = 3$ cut.

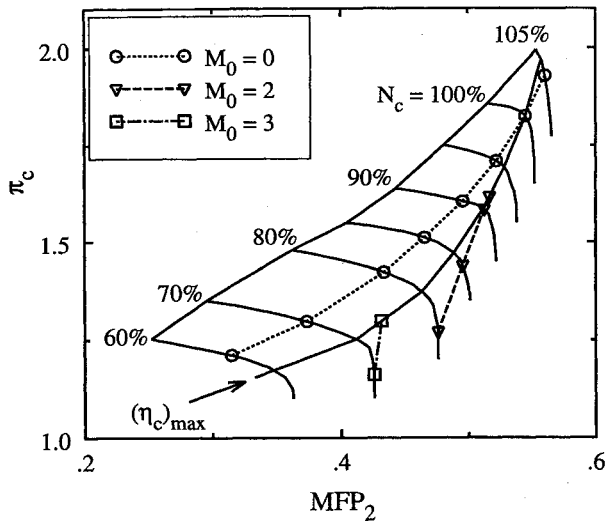


Fig. 7 Operating lines on a present-technology fan map.

in order to preserve thrust; in this case it results that the points can also fit the fan maximum efficiency line. The operating lines for the relevant nozzle area are shown. The analysis shows poor, but significant, performance. For instance, at TO conditions, F/A_2 values of about 1 and 1.1 bar can be achieved in the dry and augmented modes, respectively.

Performance

In order to highlight the engine performance capabilities, complete expansion inside the nozzle is assumed, though the authors are conscious of the impressive nozzle exit area variations that one should face along the flight path. For the same cases that have been considered in the preceding paragraph, thrust and propellant consumption have been computed, and the results are given in Figs. 8 and 9. Engine dry mode and maximum augmented mode curves are shown. Besides the specific thrust, i.e., F/m , a more direct thrust index is also given, namely the ratio F/A_2 of the thrust to the compressor inlet area, which is perhaps more interesting for assessing the engine capabilities. The thrust specific consumption is given in terms of fuel (i.e., hydrogen) consumption only. The oxygen supplied to the gas generator also contributes to the propellant consumption and should be taken into account. On the other hand, the oxygen percentage contribution is different in the engine dry or augmented mode, and a specific consumption based on both propellants could lead to a misleading evaluation of the augmented mode consumption. However, when the gas-generator MR, φ_{dry} and overall φ are known, it is easy to obtain the ratio of the overall mass flow to the hydrogen mass flow, and therefore, the ratio of the two consumption values. One should note that in the case of this study ($MR \approx 1.25$), and in the dry mode, the consumption based on both propellants is about $2.25S$.

Figure 8 gives the full throttle performance vs M_0 , i.e., the performance exhibited under the conditions shown in Fig. 4 and related to the upper points of the operating lines of Fig. 3. Relatively poor performance is obtained in the subsonic and transonic regions, due to the combined effects of the reduced compressor mechanical speed (in order to compensate for the low inlet total temperature) and of the low inlet total pressure level. This drawback is, however, related to the variations of the dynamic pressure in the initial part of the considered flight path, and could be restrained or avoided by adjusting the flight path itself. The ATR behavior is, in fact, very sensitive to the flight conditions, as can be appreciated by also examining the somewhat curious trend of the F/m and F/A_2 curves in the 0.5–1.4 range of M_0 . These curves reflect, respectively, the φ_{dry} and δ trends of Fig. 4, which are precisely related (via the compressor–turbine power balance) to the

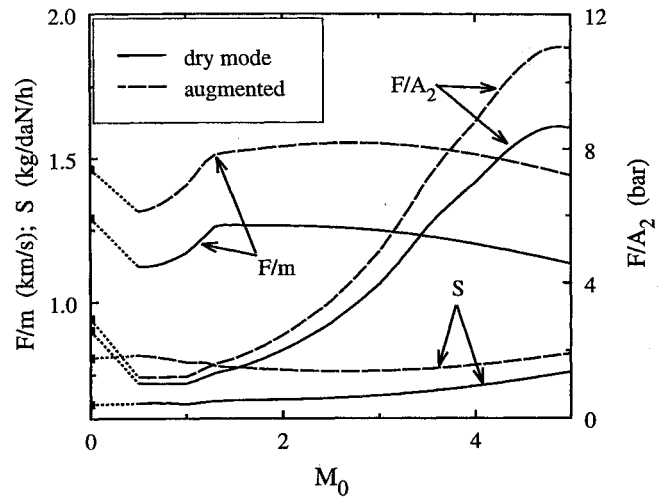
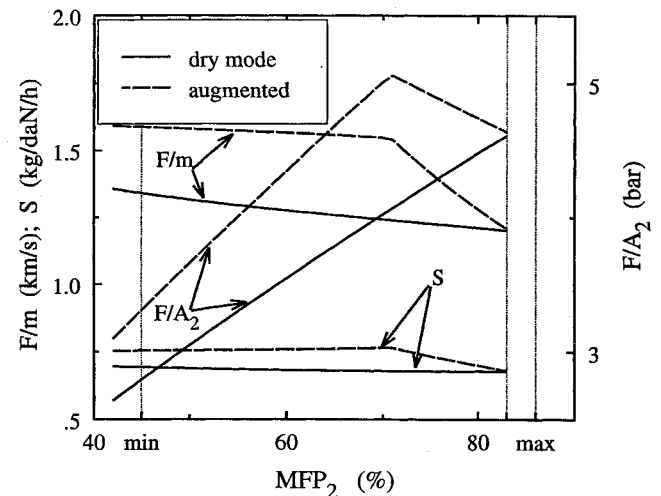


Fig. 8 Full throttle engine performance.

Fig. 9 Engine performance on the $M_0 = 3$ cut.

variation of the inlet total temperature and pressure on the flight path in that range, and to the aforementioned constraint to the compressor speed.

One should note the very impressive thrust levels that are shown at the highest M_0 . However, these may be greatly reduced by the underexpansion that a practical nozzle possibly experiences. To stress this point, one could compare the ratio of the thrust given by the simple convergent nozzle to the thrust of the adapted nozzle: at $M_0 = 5$ only a poor 50% is obtained.

Figure 9 refers to the "cut" at $M_0 = 3$, which has already been illustrated in Fig. 6. At the choking limit, which is encountered when the operating point is moved to the right, the augmented and dry modes coincide, since, in the dry mode, the nozzle throat area has been enlarged to its maximum value. By comparing the dry thrust curve with the δ curve of Fig. 6, an almost perfect proportionality can be noted. In fact, an analogous form of compensation between the factors affecting F/A_2 and δ occurs: in building up the thrust value, the increase of the air mass flow is slightly counterbalanced by the F/m decrease due to the φ_{dry} diminution; the increase of δ that is required to face the compressor power growth (proportional to the air mass flow growth) is somewhat restrained by the consequent increase of the turbine pressure ratio, and hence, of the turbine work. Incidentally, one should note that this is also the reason why φ_{dry} diminishes when moving from left to right in Fig. 6. If attention is also paid to the sensitivity of the thrust to the degree of the nozzle

expansion, then the aforementioned lessening of the specific thrust deserves more consideration. In fact, the underexpansion thrust losses are more significant, in percentage, when the specific thrust is lower. Therefore, in spite of the fact that M_0 does not vary, as neither essentially does the nozzle pressure ratio, one gets the previously mentioned thrust ratio to vary from about 80% at the left margin to roughly 65% at the choking limit on the right.

Conclusions

The off-design behavior of the air-turborocket is recognized to be very sensitive to flight conditions that are expressed by the inlet total temperature and total pressure. Different operating lines for each flight Mach number on the flight path are found.

Noticeable variations of the gas-generator pressure have to be accepted in order to maintain the operating points in the useful region of the compressor map. Attendant propellant pumping and feeding problems may therefore arise.

Advanced design compressors that allow a large airflow range are required to enhance the air-turborocket capabilities and to alleviate control problems. Variable geometry nozzles should, however, be adopted in order to exploit the compressor capabilities.

The authors are conscious that some aspects of the ATR behavior, shown by the present analysis, may to some extent depend, also qualitatively, on the assumptions that have been made. For instance, by using variable area turbine nozzles, one could restrain the otherwise impressive variations of the outlet pressure required for the GG propellant pumps. Moreover, a different choice of the design point conditions (especially as regards to the GG mixture ratio and pressure level) could result in a less-extended range of the GG propellant flow, thus reducing some control problems, and partially restoring the ATR fame to that of a "simple airbreathing engine." The general picture of the ATR behavior seems to present, however, an intrinsic degree of complexity.

Acknowledgment

This research has been supported by Ministero dell'Università e della Ricerca Scientifica e Tecnologica.

References

- ¹Hewitt, F. A., and Johnson, M. C., "Propulsion System Performance and Integration for High Mach Air Breathing Flight," *High-Speed Flight Propulsion Systems*, edited by S. N. B. Murthy and E. T. Curran, Vol. 137, Progress in Astronautics and Aeronautics, AIAA, Washington, DC, 1991, pp. 114-116.
- ²Heiser, W. H., and Pratt, D. T., *Hypersonic Airbreathing Propulsion*, AIAA Education Series, AIAA, Washington, DC, 1994, pp. 457-464.
- ³Munzberg, H. O., *Flugantriebe*, Springer-Verlag, Berlin, 1972, pp. 552-554.
- ⁴Lane, R. J., "A Review of Propulsion for High Mach Number Aircraft," *Aircraft Engineering*, Vol. 38, No. 1, 1966, pp. 11-18.
- ⁵Bendot, J. C., Brown, P. N., and Piercy, T. G., "Composite Engines for Application to a Single-Stage-to-Orbit Vehicle," NASA CR-2613, Dec. 1975.
- ⁶Cimino, P., Drake, J., Jones, J., Strayer, D., and Venetoklis, P., "Transatmospheric Vehicle Propelled by Air-Turborocket Engines," AIAA Paper 85-1373, July 1985.
- ⁷Snyder, C. A., "A Parametric Study of a Gas-Generator Airturbo Ramjet (ATR)," AIAA Paper 86-1681, June 1986.
- ⁸Lardellier, A., and Pouliquen, M., "Air Breathing Combined Engines for Space Transportation Systems," *Proceedings of the 16th Congress of the International Council of the Aeronautical Sciences*, AIAA, Washington, DC, 1988, pp. 694-700.
- ⁹Bussi, G., Colasurdo, G., and Pastrone, D., "On the Performance of the Air-Turborocket," Politecnico di Torino, Dip. di Energetica, PT-DE-MA-284, Torino, Italy, May 1992.
- ¹⁰Johnston, P. J., Whitehead, A. H., Jr., and Chapman, G. T., "Fitting Aerodynamics and Propulsion into the Puzzle," *Aerospace America*, Vol. 25, No. 9, 1987, pp. 32-37.
- ¹¹Albers, M., Eckardt, D., Kramer, P. A., and Voss, N. H., "Technology Preparation for Hypersonic Air-Breathing Combined Cycle Engines," IX International Symposium on Air Breathing Engines, Athens, Sept. 1989.